

Technische Universität Dresden • Faculty of Mathematics

# Derivation and study of a non-confluent model for deformable cells

Master's thesis

to obtain the second degree

*Master of Science*  
(*M.Sc.*)

written by

TIM VOGEL

(born on June 9, 2002 in FINSTERWALDE)

Day of submission: October 13, 2025

Supervised by Jun.-Prof. Dr. Markus Schmidtchen  
(Institute of Scientific Computing)

# **Contents**

<b>1</b>	<b>Introduction</b>	<b>5</b>
----------	---------------------	----------

## Nomenclature

abbreviation	description
PDE	A partial differential equation is an equation that contains unknown multivariable functions and their partial derivatives.
SDE	A stochastic differential equation is a differential equation in which one or more of the terms is a stochastic process, resulting in a solution that is also a stochastic process.
DF model	The discrete form model is a vertex cell model that is defined by a list of all wall points.
$N_C$	Number of cells in a model
$N_V$	Number of vertices of each cell in a model

# Mathematical conventions

---

symbol	description
$\vec{v}$	Superscript arrows denote multidimensional variables
$\frac{\partial f}{\partial v}$	Partial derivative of a scalar function $f$ with respect to a one dimensional variable $v$
$\nabla_{\vec{v}}f$	gradient $\nabla_{\vec{v}}f = (\frac{\partial f}{\partial v_1}, \dots, \frac{\partial f}{\partial v_n})^T$ , where $f$ is a scalar function and $\vec{v} = (v_1, \dots, v_n)^T$
$D_{\vec{v}}F$	Jacobian matrix $D_{\vec{v}}F = \begin{pmatrix} \frac{\partial F_1}{\partial v_1} & \dots & \frac{\partial F_1}{\partial v_n} \\ \vdots & & \vdots \\ \frac{\partial F_m}{\partial v_1} & \dots & \frac{\partial F_m}{\partial v_n} \end{pmatrix}$ , where $\vec{v} = (v_1, \dots, v_n)^T$ is a multidimensional variable and $F = (F_1, \dots, F_m)^T$ is a vector valued function
$\Delta f$	Laplacian of a scalar function $f$
$2e - 3$	scientific notation for $2 \times 10^{-3} = 0.002$

---

# 1 Introduction

Collective cell migration represents a fundamental process underpinning various biological phenomena, including embryonic development, tissue regeneration, wound healing, and the invasive potential of certain cancers. The collective nature of cell movement has been acknowledged for over a century, with early observations recognising its importance in developmental and regenerative processes [AT20, Hol14, Her32, VT66]. However, the underlying mechanisms driving this coordinated behavior remained contentious, with competing hypotheses suggesting roles for pressure [Her32], surface tension [AT20], or active forces generated by leading cells [Hol14]. Following a period where research emphasis shifted towards molecular and genetic details, the field has witnessed a resurgence of interest in understanding the physical principles governing collective cell migration. This revival is largely attributed to recent advances in experimental techniques [RCCT17, DRSB<sup>+</sup>05, TWA<sup>+</sup>09], enabling direct measurements of mechanical forces exerted by cells, and the development of new conceptual frameworks in biophysics and active matter physics [MJR<sup>+</sup>13, PJJ15, JGS18], which challenged purely reductionist perspectives [GT18]. These developments coincided with a growing recognition of the critical role of collective cell migration not only in physiological processes but also in the progression of malignant diseases [FNW<sup>+</sup>95].

The diverse manifestations of collective cell migration depend heavily on the specific biological context and tissue type [FG09]. For instance, epithelial cells often migrate as cohesive sheets on the extracellular matrix (ECM) during morphogenesis, wound closure, and regeneration. Snapshots from a cell wound healing process, illustrating the dynamics of cell migration, are shown in Figure 1.

In contrast, cancer cells often invade tissues as sheets, strands, or clusters, navigating a complex three-dimensional extracellular matrix (ECM) environment [FG09, CCP<sup>+</sup>14, CV15].

While cell migration occurs extensively in three dimensions, modeling these complex processes remains a significant challenge. Consequently, much current scientific work focuses on two dimensional systems as a more tractable approach to understand the underlying physical principles. Throughout this thesis, we consider cell dynamics within a bounded two-dimensional domain, denoted by  $\Omega \subset \mathbb{R}^2$ . Throughout this work, the total number of cells present within the domain  $\Omega$  is denoted by  $N_C \in \mathbb{N}$ . In two dimensions, cell monolayers serve as fundamental model systems to study cell behavior and tissue function. These systems, comprising a single layer of cells grown on a surface, can be mathematically and computationally modeled in either a confluent or non-confluent manner. A confluent cell model depicts a continuous, tightly packed layer where cells cover the entire surface without gaps, whereas a non-confluent monolayer represents a state with spaces and gaps between individual cells or cell clusters that have not yet achieved full surface coverage.

Recent years have seen growing interest in understanding the principles governing collective cell migration in confluent cell monolayers and epithelial tissues, which exhibit remarkable patterns and correlations in both structural arrangements and actively driven flows [WV21]. Experimental studies on model systems have revealed phenomena such as unjamming transitions, spontaneous vortex formation, topo-

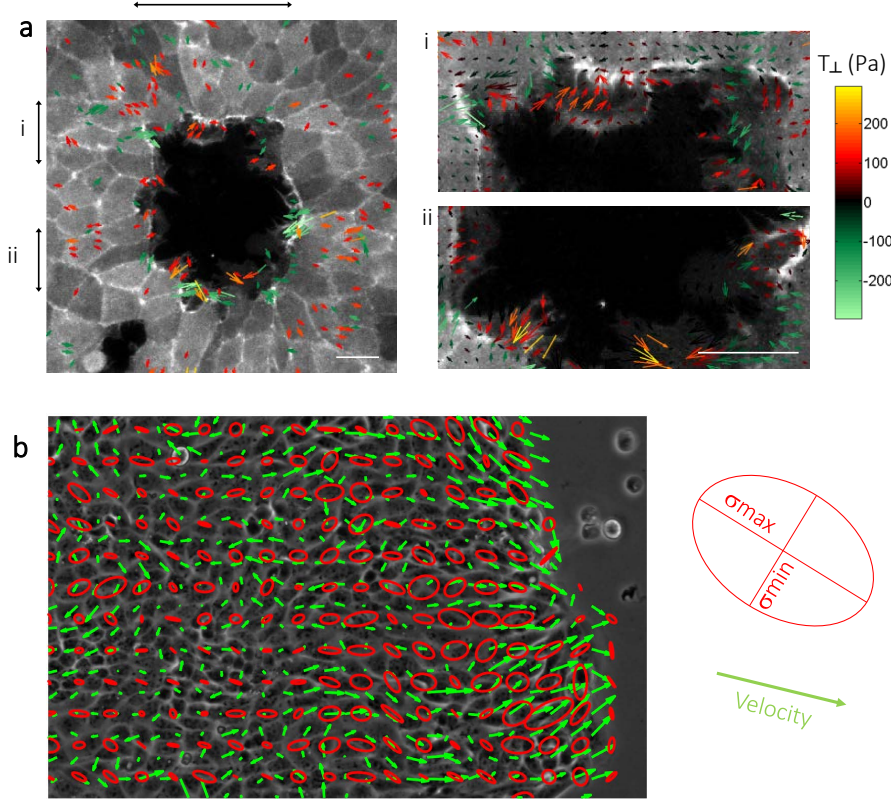


Figure 1: A figure from the paper [AT20] illustrating cell migration during the wound healing process. (a) Vector field representation of cellular traction forces in cells as they close a wound, with color intensity reflecting the radial component (positive values indicate outward-directed forces). Panels labeled i and ii present magnified views of the regions marked by arrows in panel (a). (b) Velocity vectors (green) and monolayer stress ellipses (red), depicting the principal stress directions and magnitudes, in a growing cell colony (phase contrast).

logical defects, and active turbulence. A key challenge is linking this macroscopic behavior to the properties of individual cells and their interactions, leading to a diverse range of modeling approaches spanning different levels of coarse-graining, from subcellular lattices and multiphase field models to vertex, Voronoi, particle, and continuum models. The systematic comparison of these diverse cell models is crucial for selecting appropriate methods for future studies and enabling predictive simulations of patterns and correlations in cell colonies.

Understanding the diffusion behavior of cells, influenced by various forces and interactions, is a key aspect of collective cell migration. This will be a central focus of this thesis. Different mathematical cell models, incorporating distinct cell dynamics, will exhibit varying diffusion behaviors. To begin this investigation, we will first introduce the simplest model: the point particle model.

### Point particle model

We consider the point particle model on a two dimensional bounded domain  $\Omega \subset \mathbb{R}^2$ , where we have  $N_C \in \mathbb{N}$  particles. These particles have no real size. There is also no

particle interaction, as there is no possibility of collision.

Initially, the particles are randomly distributed in  $\Omega$ .

The particles' dynamics are governed solely by Brownian motion. Brownian motion is a random and unpredictable motion that occurs in the real world when particles are suspended in a fluid and collide with surrounding molecules.

In mathematics, we model Brownian motion using stochastic differential equations (SDEs), which are equations that describe the motion of a particle over time in a random and unpredictable manner. SDEs are a powerful tool for modeling complex phenomena in physics, finance, and other fields, and are characterized by the presence of random terms that capture the uncertainty of the system.

Let

$$\vec{x}_i(t) \in \Omega \quad 1 \leq i \leq N,$$

be the location of the particle  $i$  at time  $t > 0$ . The particle movement can be modeled using the diffusion equation, which describes the random motion of particles over time

$$d\vec{x}_i(t) = \sqrt{2D} dB_t^{(i)}, \quad 1 \leq i \leq N,$$

where the constant  $D > 0$  represents the diffusion coefficient which proportionally scales the speed of the particle movements by scaling the random fluctuations. The term  $dB_t^{(i)}$  introduces the randomness of Brownian motion, where  $dB_t^{(i)}$  is a normally distributed random variable that accounts for the unpredictable changes in the position of particle  $vecx_i$  over time.

We also consider the probability density function  $\rho(t, \vec{x})$ , which describes the probability of finding a particle at a specific position  $\vec{x}$  at time  $t$ . In the given context, the function  $\rho$  satisfies the partial differential equation:

$$(1) \quad \frac{\partial \rho(t, \vec{x})}{\partial t} = D \Delta_{\vec{x}} \rho(t, \vec{x}),$$

where  $\Delta_{\vec{x}}$  is the Laplacian operator with respect to the spatial variables.

Equation (1) represents the classic diffusion equation, a cornerstone of physics and mathematics. The same diffusion constant  $D > 0$  is used in the SDE for particle movement and the PDE for the probability density function  $\rho$ .

### Hard sphere model

Next, we consider models that add a real size to the particles and introduce particle interactions. With the inclusion of a real size, the particles cannot overlap, resulting in exclusion effects. To account for this, we introduce a new interaction dynamics that ensures the particles do not overlap. This new interaction dynamics leads to a more complex and realistic model that captures the behavior of particles with a real size and interactions.

Since particles cannot overlap, the domain  $\Omega_\epsilon^{(i)}$ , that holds the information where the centre of particle  $i$  can be located, must exclude the areas where  $\|\vec{x}_i - \vec{x}_j\|_2 \leq \epsilon$  for all  $1 \leq j \leq N_C$ ,  $j \neq i$ . This is due to the fact that particles cannot occupy the same space simultaneously.

The domain that holds all possible locations of the particles is then given by

$$\Omega_\epsilon^{N_C} = \Omega_\epsilon^{(1)} \times \dots \times \Omega_\epsilon^{(N_C)}.$$

This can be visualized as a product space, where each particle's domain is combined to form a larger domain that encompasses all possible locations of the particles. Under this circumstances, we will get a new dynamic compared to the point particle model. Figure 2 illustrates how a hard sphere cell configuration looks like compared to a point particle configuration.

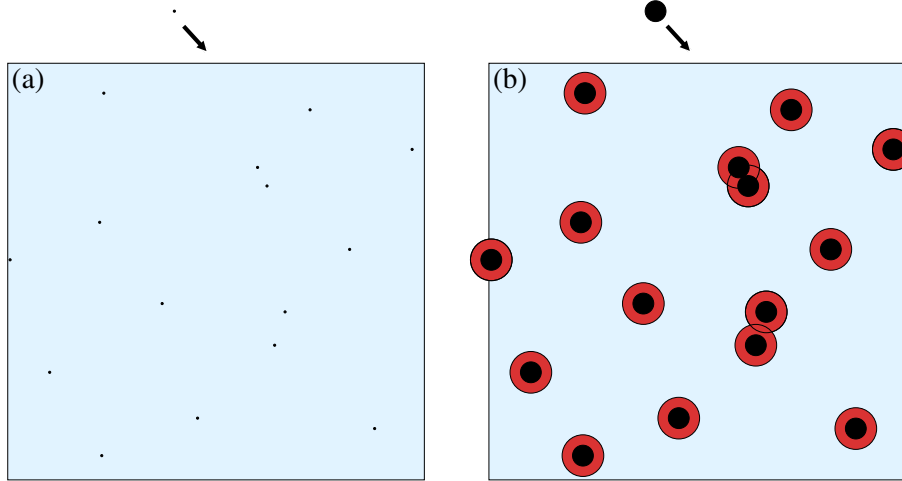


Figure 2: An illustration from [BC12] of the point particles on the left and the hard sphere particles on the right. We can see areas where the centre of the particles cannot be located, as they would overlap with other particles being marked red.

In the work of Bruna et al. [BC12], a hard sphere particle model is examined. Here, the particles are spherical in shape, with a diameter  $0 < \epsilon \ll 1$ . All particles in this model are distinct and can be distinguished from one another. The diffusivity constant  $D$  is set to be  $D = 1$ .

The hard sphere model is characterized by the fact that any interaction between particles may cause a change in their direction of motion, but the spherical shape of the particles remains unchanged. Hardcore collisions are modeled as reflective boundary conditions on the collision surfaces defined by  $r = \|\vec{x}_i - \vec{x}_j\|_2 = \epsilon$ , where  $1 \leq i < j \leq N_C$ . The external forces acting on a particle in the system are described by the force function  $f : \mathbb{R}^2 \rightarrow \mathbb{R}^2$ , which depends only on the location of the particle. The function  $\vec{F}$  maps the particle configuration  $\vec{X} = (\vec{x}_1, \dots, \vec{x}_{N_C})^T$  to the vector of external forces  $\vec{F}(\vec{X}) = (f(\vec{x}_1), \dots, f(\vec{x}_{N_C}))^T$ . The dynamics of the particles are governed by the SDE

$$d\vec{x}_i(t) = \sqrt{2D} dB_t^{(i)} + f(\vec{x}_i(t)) dt, \quad 1 \leq i \leq N_C.$$

In this model, the particles are initially randomly distributed in  $\Omega_\epsilon^{N_C}$ , ensuring that no overlap occurs between the particles. The joint probability density function  $P$  of the  $N_C$  particles satisfies the high-dimensional Fokker-Planck equation

$$\frac{\partial P}{\partial t} = \nabla_{\vec{X}} \cdot (\nabla_{\vec{X}} P - P \vec{F}),$$

where  $\nabla_{\vec{X}}$  and  $\nabla_{\vec{X}} \cdot$  denote the gradient and divergence operators with respect to the  $N_C$ -particle position vector  $\vec{X}$ .

Using the method of matched asymptotic expansions, the authors also derived the probability density function  $\rho$  of finding a single particle at time  $t$  and position  $\vec{x}$ , which satisfies the equation

$$(2) \quad \frac{\partial \rho(t, \vec{x})}{\partial t} = \Delta_{\vec{x}} \rho + \frac{\pi}{2} (N_C - 1) \epsilon^2 \Delta_{\vec{x}} (\rho^2) - \nabla_{\vec{x}} \cdot (f(\vec{x}) \rho).$$

When  $f$  is neglected and  $\epsilon \rightarrow 0$ , this equation reduces to the probability density function of the point particle model, except for a rescaling factor. The Fokker-Planck equation is a direct extension of the diffusion equation, with an additional drift term.

A central finding of [BC12] is shown in Figure 3, which compares the diffusion behavior of the point particle model and the hard sphere model.

### Soft sphere model

Next, we consider an extension of the model by introducing deformable soft spherical particles. This new model incorporates the effect of deformation and interaction between particles through a potential energy function that depends on the distance between the particles. The paper [BCR17], written by Bruna, Chapman and Robinson, analyses the diffusion properties of such a model.

In contrast to the soft sphere model, the hard sphere model enforces rigid, non-deformable cell boundaries through reflective boundary conditions at a fixed separation distance, leading to abrupt, instantaneous collisions without any interface deformation. The soft sphere model uses a smoother approach including interaction potentials.

The equation of motion for each particle  $i$  is given by

$$d\vec{x}_i(t) = \sqrt{2D} dB_t^{(i)} + f(\vec{x}_i(t)) dt - \sum_{j \neq i} \nabla_{\vec{x}_i} u(\|\vec{x}_i(t) - \vec{x}_j(t)\|_2) dt, \quad 1 \leq i \leq N_C,$$

where  $\nabla_{\vec{x}_i}$  is the gradient with respect to  $\vec{x}_i$ .

The effect of the interaction potential is to cause particles to repel or attract each other depending on the distance between them, rather than simply overlapping.

For the modeling of short range interacting soft sphere particles, the authors computed the one particle probability density  $\rho(t, \vec{x})$  of finding a given particle at position  $\vec{x}$  at time  $t$  developing according to

$$(3) \quad \frac{\partial \rho}{\partial t} = \nabla_{\vec{x}} \cdot (D \nabla_{\vec{x}} \rho - f(\vec{x}) \rho + \alpha_u \epsilon_u^2 (N_C - 1) \rho \nabla_{\vec{x}} \rho)$$

where  $\alpha_u$  depends on the interaction potential  $u$  and  $0 < \epsilon_u \ll 1$  is the interaction range of  $u$ . When comparing the first marginals of the soft sphere model (Equ. (3)) and the hard sphere model (Equ. (2)), we can see that they are similar in structure, with the main difference being the coefficients of the nonlinear diffusion terms. We can not clearly say which model diffuses faster, as this is dependent on the modelling of the soft interaction.

The influence of the cell hardness to the diffusion rate of the cell system will be investigated in this thesis. We even introduce a parameter that can continuously change the cell hardness from hard to soft.

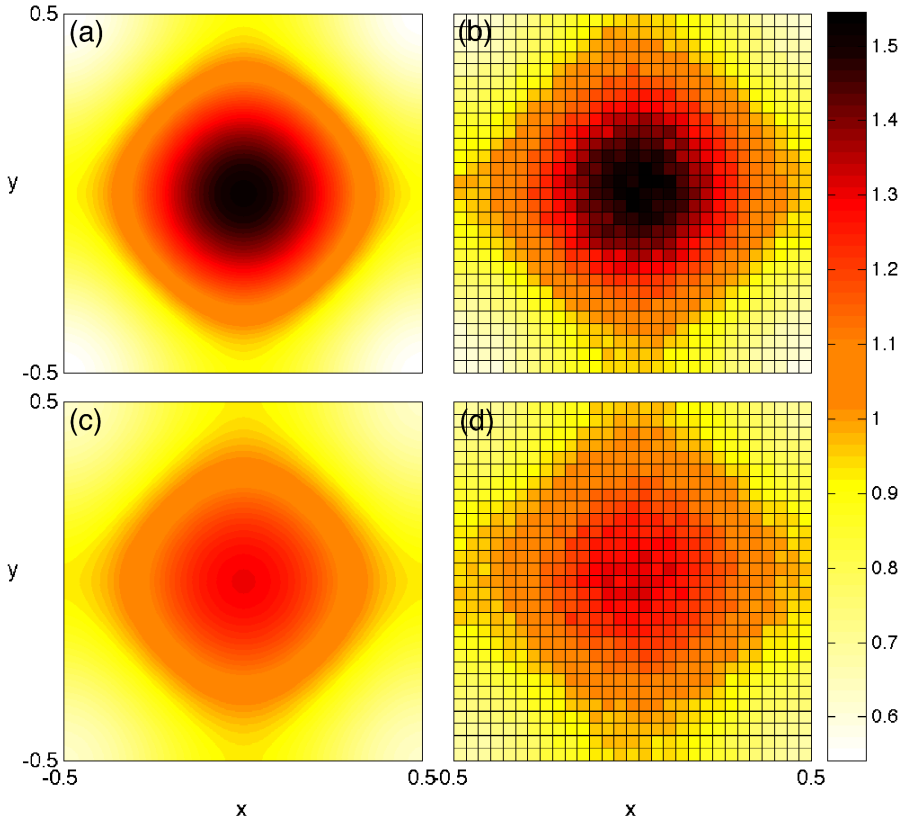


Figure 3: This figure from [BC12] contains the following four plots, all of them are shown at time  $t = 0.05$ . For all plots, the initial condition is normally distributed with mean  $(0, 0)^T$  and standard deviation 0.09. (a) shows the solution of the linear diffusion Equation (1) for point particles. (b) shows the histogram of a Monte Carlo simulation of the point particle model. (c) shows the solution of the nonlinear diffusion Equation (2) for finite-sized particles. (d) shows the histogram of a Monte Carlo simulation of the hard sphere model. The Monte Carlo simulations used  $10^4$  simulation runs each with a time step size of  $10^{-5}$ . We can see that the hard sphere model in (c) and (d) shows a quicker diffusion rate as the cell concentration in the centrum of the domain has already diffused more compared to the point particle model in (a) and (b).

While these models are powerful, they are limited to spherical particles and do not account for the complex shapes and deformations observed in biological cells.

### Phase field models

A new cell modeling framework is now considered. The phase field approach exhibits conceptual parallels with the soft sphere model proposed by Bruna, Chapman, and Robinson [BCR17], particularly in how cell-cell interactions are modeled through a continuous repulsive energy that prevents overlap. In both formulations, interactions are governed by a smooth, short range influence manifesting through the diffuse interface in the phase field model and via the interaction potential  $u$  in the soft-sphere model, thereby enabling a realistic description of cell crowding effects.

Nevertheless, the phase field model diverges fundamentally in its underlying structure: it is a continuum model based on partial differential equations that explicitly encodes cell morphology and internal organisation through the phase field variable  $\phi_i$ , enabling dynamic shape changes, topological transitions, and coupling to geometric features such as surface curvature. In both models, the interaction mechanism operates continuously and locally, ensuring a seamless transition between overlapping and non overlapping configurations while maintaining physical consistency.

The soft-sphere model derives its interaction dynamics from the potential energy  $u(\|\vec{x}_i - \vec{x}_j\|_2)$ , which leads to a nonlinear diffusion equation featuring a diffusion coefficient that depends on local density. Analogously, in the phase field model, the interaction energy emerges from a non-local term in the free energy functional, producing a repulsive force between cells that scales with the local concentration of  $\phi_i$ . These shared mathematical features: gradient flow evolution, continuous interaction laws and density-dependent diffusion underscore a formal and conceptual alignment between the two approaches.

Although the phase field model inherits key principles from the soft-sphere model, such as continuous interaction and density-dependent transport, it fundamentally differs from both the soft-sphere and hard-sphere frameworks in its physical representation. The phase field model resolves cell overlaps through a free energy which enables gradual, continuous deformation of cell interfaces, thereby avoiding discontinuities in the dynamics that are characteristic of discrete collision models.

The free energy functional encodes shape regularization, intercellular interactions, and physical constraints of the system. Unlike the soft-sphere model, which treats cells as point-like entities interacting via a smooth potential, the phase field model represents cells as much more complex, spatially extended, continuously structured entities, with their internal state fully described by the evolution of the phase field variable  $\phi_i$ . This enables a natural description of complex cell morphologies, topological transitions such as cell division or fusion, and the integration of cell mechanics with geometric curvature via extrinsic curvature contributions in the free energy.

Phase field variables represent cells as smooth functions  $\phi_i(\vec{x}, t) \in [-1, 1]$ , with  $\phi_i > 0$  in the cell interior and  $\phi_i < 0$  in the exterior. The cell wall is denoted by values of  $\phi_i = 0$ . An illustration of a phase field variable is shown in Figure 4.

The dynamics of  $\phi_i$  are governed by a gradient flow of a free energy functional:

$$\frac{\partial \phi_i}{\partial t} + v_0(\vec{v}_i \cdot \nabla_{\vec{x}} \phi_i) = \Delta_{\vec{x}} \frac{\delta F}{\delta \phi_i}, \quad 1 \leq i \leq N_C$$

where  $\vec{v}_i$  is a vector field used to incorporate activity, with a self propulsion strength  $v_0$ ,  $F$  is a free energy, and  $\frac{\delta F}{\delta \phi_i}$  denotes the first variation.

The free energy  $F$  arises from a sum of different energies,

$$F = F_{CH} + F_{INT} + F_M.$$

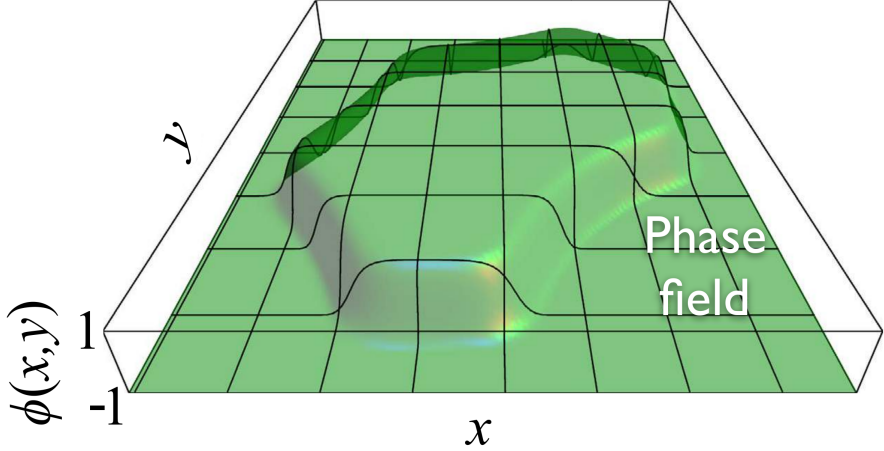


Figure 4: A snapshot from the paper [AT20] illustrating a phase field variable. The cell's inside has value  $\phi = 1$  and the outside  $\phi = -1$ .

The first energy is a Cahn-Hilliard energy and could look like in [WV21]

$$F_{CH} = \sum_{i=1}^N \int_{\Omega} \frac{1}{Ca} \left( \frac{\epsilon}{2} \|\nabla_{\vec{x}} \phi_i\|_2^2 + \frac{1}{\epsilon} W(\phi_i) \right) d\vec{x},$$

$\epsilon$  is a small parameter related to the interface thickness, and  $Ca$  is a capillary number that scales the relative importance of surface tension. The term  $\|\nabla_{\vec{x}} \phi_i\|_2^2$  penalises a long cell wall, as  $\nabla_{\vec{x}} \phi_i \neq 0$  only at the cell wall.  $W(\phi_i) = \frac{1}{4}(\phi_i^2 - 1)^2$  is a double-well potential. This energy ensures that each  $\phi_i$  maintains a stable interface of  $[-1, 1]$ . The second energy term  $F_{INT}$  models cell-cell interactions and could be defined as in [WV21]

$$F_{INT} = \sum_{i=1}^N \frac{1}{Ca} \int_{\Omega} B(\phi_i) \sum_{j \neq i} w(d_j) d\vec{x},$$

where

$$B(\phi_i) = \frac{3}{4\sqrt{2}\epsilon} (\phi_i^2 - 1)^2$$

is an approximation of the delta function of the cell boundary that is non-zero only at the cell wall. The sum in the integral accounts for the interaction with all other cells  $j \neq i$  through a short-range potential  $w(d_j)$ , where  $d_j$  is the signed distance function to the cell boundary of cell  $j$ .

The third energy term  $F_M$  differs for different models and incorporates additional mechanical properties of the cells, such as area conservation or bending energy.

- In [WV21], the authors focussed on the influence of microscopic details to incorporate active forces on emerging phenomena. The models are based on cell deformations and cell-cell interactions and we investigate - We compare four different approaches, one in which the activity is determined by a random orientation,

one where the activity is related to the deformation of the cells, and two models with subcellular details to resolve the mechanochemical interactions underlying cell migration. - The models are compared with respect to generic features, such as coordination number distribution, cell shape variability, emerging nematic properties, as well as vorticity correlations and flow patterns in large confluent monolayers and confinements. - The random model determines the direction of motion on the single cell level by a stochastic process - elongation model aligns the direction of motion with the long axis of the cell - polar and a nematic model, which use subcellular details to determine strength and direction of motion on a single cell level.

- The goal of this paper is a systematic comparison of these approaches and their linkage with statistical observables of experiments to provide a route towards predictive simulations of patterns and correlations in cell colonies. After introducing the multiphase field models, discussing microscopic differences, and briefly describing the numerical approach enabling large-scale simulations, we address coordination number distribution, analyze statistics on shape variability of the cells and the ratio of multicellular rosettes, velocity distributions of emerging topological defects, their stress fields, as well as defect density and creation rates - All results are compared with experimental data for a large variety of cell cultures. The appearing qualitative differences of the models show the importance of microscopic details.

characteristic	Random	Elongation	Polar	Nematic
Coordination number distribution	(✓)	(✓)	(✓)	(✓)
Shape variability	(✓)	✓	✓	(✓)
Rosette ratio	Differences between models			
Velocity distribution of topological defects	Differences between models			
Correlation between direction of motion and orientation of defect	✗	✓	✓	(✓)
Elastic property of + 12 defect	✗	Extensile	Contractile	Contractile
Active turbulence	(✓)	(✓)	(✓)	(✓)
Vorticity-vorticity correlation	Similar for all models			
Dependency of defect density on activity	Linear	Linear	Linear	Constant
Rotational motion in circular confinement	✗	(✓)	✗	✗

Table 1: Comparison of the four different phase field models from [WV21] with respect to various characteristics observed in experiments. A check mark ✓ indicates observed agreement, ✗ indicates disagreement and (✓) indicates only qualitative agreement with universal feature. If experimental data are not available or insufficient for a comparison, only similarities or differences of the models are noted.

- Another work that uses phase field models to describe cell dynamics is [HV23] by

Axel Voigt and Lea Happel. - this work focuses on the impact of curved domains on the collective behavior of cells, defining the phase fields on tori. - it focuses on emergent collective behaviors such as coordinated rotation on curved surfaces, driven by curvature alignment and self-propulsion. - while the soft-sphere model typically assumes spherical symmetry and isotropic interactions, the phase field model can incorporate anisotropic effects—such as alignment with principal curvature directions—through geometric coupling terms, enabling the simulation of complex collective behaviors like coordinated rotation on curved surfaces. These differences make the phase field model more biologically realistic for epithelial tissues, but also more computationally demanding than the simpler point-particle approaches. - The phase field model developed by Happel and Voigt [?] demonstrates that extrinsic curvature coupling is essential for explaining the alignment of cell elongation with principal curvature directions and the emergence of coordinated rotational motion in epithelial layers on curved surfaces. Their simulations reproduce key experimental observations—such as spontaneous rotation on cylinders and curvature-dependent shape changes on tori—by combining a diffuse interface representation with a free energy that includes both intrinsic and extrinsic geometric terms. This work underscores the importance of geometric effects in tissue morphogenesis and provides a framework for studying how curvature influences collective cell behavior beyond flat, two-dimensional environments.

### Vertex models

With precedents in the physics of foams, network models describe epithelial tissues as networks of polygonal cells. Thus, albeit in less detail than lattice and phase-field models, these models still describe subcellular features of cell shape. They encompass two subtypes of models: vertex and Voronoi models.

- In vertex models, the degrees of freedom are the vertices of the polygons. - Alternatively, the network can be described by the cell centers, and this reduces the number of degrees of freedom. These descriptions are known as Voronoi models because, given the positions of the cell centers, the cell-cell boundaries are delineated by the Voronoi tessellation - The difference in the number of degrees of freedom has important consequences for the mechanical properties of the network, which may thus differ between vertex and Voronoi models - In Voronoi models, the network is dynamic, evolving with each recomputation of the tessellation - In vertex models, by contrast, network rearrangements entail the appearance and disappearance of vertices, which requires implementing specific rules

- the paper [BSY<sup>+</sup>18] by Boromand, Merkel and Manning, studies the jamming transition in a system of deformable cells with a vertex model. - what's interesting for us is its the non-confluent cell model - the particle model is called deformable particle (DP) model - it can be used to model cells, foams, emulsions, and other soft particulate materials - The DP model combines the ability to model individual soft particles with the shape-energy function of the vertex model, - there is a shape-energy function that is minimized for area and perimeter and repulsive interparticle forces. - we have: \* p perimeter \* a area \* bond vector  $\vec{l}_{mi}$  connects vertices  $i$  and  $i + 1$  of cell  $m$  that are written as  $\vec{v}_{m,i}$  and  $\vec{v}_{m,i+1}$ , respectively. - shape energy

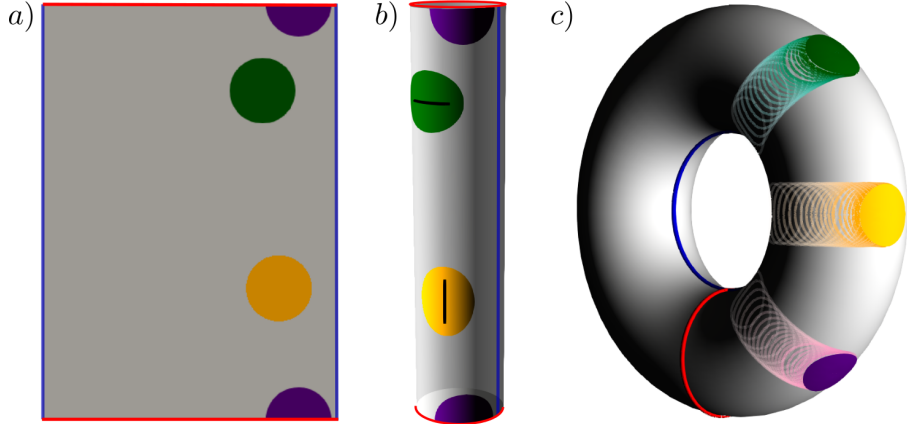


Figure 5: A figure from the paper [HV23] showing a phase field variable  $\phi$  on a curved domain, specifically a torus. In (a) and (b), the surface of the torus from (c) is shown as a parametrization on a rectangle, where the blue edges are identified (glued together) to form the toroidal direction, and the red edges are similarly identified to form the poloidal direction. Red and blue lines represent periodic boundary conditions, which are enforced by gluing the corresponding edges in (b) and (c). The color coding corresponds to the extrinsic curvature parameter  $E_c$  (see Eq. (3)):  $E_c = 0$  (purple) results in a geodesic circle on both geometries;  $E_c > 0$  (green) favors alignment with the direction of maximum absolute curvature;  $E_c < 0$  (yellow) favors alignment with the direction of minimal absolute curvature. Cell elongation is highlighted for visibility. On toroidal surfaces, cell shape depends on position due to varying curvature. (c) shows the trajectories, final positions, and shapes of cells over time. The influence of extrinsic curvature is not apparent in the final configuration, as all shapes were obtained by solving Eq. (1) with  $v_0 = 0$ .

function:

$$U = U_{contract} + U_{compress} + U_{linetension} + U_{bending} + U_{interaction},$$

$$U_{contract} = \frac{k_l N_v}{2} \sum_{m=1}^N \sum_{i=1}^{N_v} (l_{m,i} - l_0)^2,$$

where  $N_v$  number of vertices per cell,  $k_l$  is spring constant,  $l_0$  equilibrium length of the edges

$$U_{compress} = \frac{k_a}{2} \sum_{m=1}^N (a_m - a_0)^2,$$

where  $k_a$  is compressibility constant,  $a_0$  equilibrium area of the cell

$$U_{linetension} = \gamma \sum_{m=1}^N \sum_{i=1}^{N_v} l_{m,i},$$

where  $\gamma$  is the line tension coefficient,

$$U_{bending} = \frac{k_b}{2N_v} \sum_{m=1}^N \sum_{i=1}^{N_v} \left( \frac{2(\hat{l}_{m,i} - \hat{l}_{m,i+1})}{l_{m,i} - l_{m,i+1}} \right)^2,$$

where the last sum is a cyclic summation,  $k_b$  is the bending rigidity constant,  $\hat{l}_{m,i} = \frac{\vec{l}_{m,i}}{\|\vec{l}_{m,i}\|_2}$  is the unit vector of  $\vec{l}_{m,i}$

There are two different methods to model the repulsive interaction between two deformable polygons called rough surface (RS) and smooth surface (SS) method. - In the RS method, each vertex of a polygon is treated as the center of a disk with diameter  $\delta = l_0 = 1$ . - Repulsive interactions are computed as linear spring forces between overlapping disks on contacting polygons. - This method effectively models a "rough" surface with discrete, localized repulsion at vertices.

$$U_{RSinteraction} = \sum_{m=1}^N \sum_{n>m}^N \sum_{j=1}^{N_v} \sum_{k=1}^{N_v} \frac{k_r}{2} (\delta - |\vec{v}_{m,j} - \vec{v}_{n,k}|)^2 \times \Theta(\delta - |\vec{v}_{m,j} - \vec{v}_{n,k}|),$$

where  $k_r$  is the repulsive constant,  $\delta$  is the diameter of the disks or width of the circulo-lines (see Fig. 6), and  $\Theta$  is the Heaviside step function, that is either 1 for a positive argument or 0 otherwise.

- In contrast, the SS method models polygon edges as circulo-lines (i.e., line segments with finite width  $\delta$ ). - The repulsive interaction is computed based on the minimum distance  $d_{min}$  between two edge segments  $l_{m,j}$  and  $l_{n,k}$ , replacing the vertex-to-vertex distance in the RS method. The interaction energy becomes:  $U_{SSinteraction} = \sum_{m=1}^N \sum_{n \neq m} \sum_{j=1}^{N_v} \sum_{k=1}^{N_v} \frac{1}{2} k_r (\delta - d_{min})^2 \Theta(\delta - d_{min})$ , where  $d_{min}$  is the shortest distance between the two line segments. This method provides a smoother, more continuous repulsion, better approximating the behavior of soft, continuous interfaces.

Despite the different interaction mechanisms, both methods yield similar structural and mechanical properties at jamming onset. This indicates that the overall jamming behavior is robust to the specific choice of interaction model. Figure 6 illustrates the two interaction methods.

A simpler approach for modeling diverse shapes in cell models is to use a vertex-based model, as used in [FOBS14]. Vertex models are a valuable tool in computational biology and biophysics for studying the biomechanics and behavior of cells and tissues.

In a vertex model of a cell, the cell's outline or boundary is approximated as a polygon, with the vertices of this polygon representing discrete points along the cell's boundary. Movements or transformations of the cell are given by forces that are applied on each vertex individually.

The cell dynamic in a vertex model is given by the equation

$$(4) \quad \eta \frac{d\vec{x}_i}{dt} = F_i, \quad 1 \leq i \leq N,$$

where  $\eta$  is a scaling factor and  $F_i$  is the total force acting on  $\vec{x}_i$ .

Like in the phase field model,  $F_i$  is a sum of different forces that define the cell

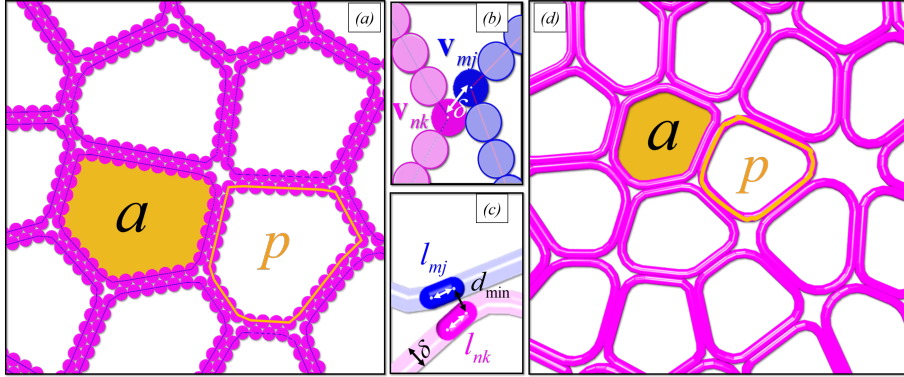


Figure 6: A snapshot from the paper [BSY<sup>+</sup>18] illustrating a configuration of vertex-based deformable cells. Schematic of deformable polygons with  $N_v = 34$  vertices (where the position of the  $j$ -th vertex in the  $m$ -th polygon is denoted by  $\vec{v}_{m,j}$ ), area  $a_m$ , and perimeter  $p_m$ . The edge  $l_{m,j} = p_m/N_v$  represents the line segment connecting vertices  $j$  and  $j + 1$  in polygon  $m$ . Two methods are used to model the edges of deformable polygons: (a) and (b) show the RS method, where disks of diameter  $\delta$  are centered at the polygon vertices; (c) and (d) show the SS method, where polygon edges are modeled as circulo-lines of width  $\delta$ . The quantity  $d_{\min}$  denotes the minimum distance between the line segments  $l_{m,j}$  and  $l_{n,k}$ .

behavior, such as the cell flexibility or the interaction with other cells.

Our new cell model shall be able to represent a wide range of shapes, similar to the phase field model in [HV23] and the vertex model in [FOBS14].

- we have worked on the same 4 forces as in this thesis, but in the master thesis, there were many adaptations made - bug fixes, redefining forces with neighboring vertices, stability - parameter studies to find force scalings that work - parallelisation of the code to be able to run the monte carlo sims

### Discrete form model

- our model is also vertex based, but we use it in a non confluent setting - we can use different desired shapes - cell deformation is allowed - shape preserving forces and interaction forces - transition from hard discs to soft discs and then other shapes

The DF model shares several key features with the referenced cell models. All frameworks after the point particles account for excluded-volume effects, which prevent cell overlap and lead to enhanced diffusion and non-trivial collective behavior. The dynamics in each model are governed by gradient flows of energy functionals, ensuring that the system evolves toward lower-energy configurations. Furthermore, stochastic motion—modeled as Brownian motion—is included in all approaches to capture thermal fluctuations. These shared principles provide a strong foundation for comparing our model to established frameworks. Like the vertex model of Fletcher et al. [FOBS14], our cells are represented as polygons with discrete vertices, and their dynamics are governed by forces derived from energy gradients. However, unlike the standard vertex model, our framework explicitly incorporates a \*\*hardness parameter  $h \in [0, 1]$ \*\* that allows for a continuous transition from rigid hard-sphere behavior ( $h = 1$ ) to fully deformable cell dynamics ( $h = 0$ ). In this thesis, we derive and study a non-confluent DF model that systematically investigates

how cellular deformability—controlled by the hardness parameter  $h$ —influences the overall diffusivity of the cell system. By connecting our model to the established frameworks of Bruna and Chapman [BC12, BCR17] and Happel and Voigt [HV23], we provide a unified perspective on cell dynamics that spans from rigid to deformable regimes.

- we define similar energies as in [FOBS14], but we mostly consider simulations with only  $N_V = 6$  vertices per cell.

## **Statement of authorship**

I hereby declare that I have written this thesis (*Derivation and study of a non-confluent model for deformable cells*) under the supervision of Jun.-Prof. Dr. Markus Schmidtchen independently and have listed all used sources and aids. I am submitting this thesis for the first time as part of an examination. I understand that attempted deceit will result in the failing grade „not sufficient“ (5.0).

---

Tim Vogel

Dresden, October 13, 2025

Technische Universität Dresden

Matriculation Number: 4930487

## References

- [AT20] Ricard Alert and Xavier Trepat. Physical models of collective cell migration. *Annual Review of Condensed Matter Physics*, 11(1):77–101, 2020.
- [BC12] Maria Bruna and S. Jonathan Chapman. Excluded-volume effects in the diffusion of hard spheres. *Phys. Rev. E*, 85:011103, Jan 2012.
- [BCR17] Maria Bruna, S. Jonathan Chapman, and Martin Robinson. Diffusion of particles with short-range interactions. *SIAM Journal on Applied Mathematics*, 77(6):2294–2316, 2017.
- [BSY<sup>+</sup>18] Arman Boromand, Alexandra Signoriello, Fangfu Ye, Corey S. O’Hern, and Mark D. Shattuck. Jamming of deformable polygons. *Phys. Rev. Lett.*, 121:248003, Dec 2018.
- [CCP<sup>+</sup>14] Danfeng Cai, Shann-Ching Chen, Mohit Prasad, Li He, Xiaobo Wang, Valerie Choesmel-Cadamuro, Jessica K Sawyer, Gaudenz Danuser, and Denise J Montell. Mechanical feedback through e-cadherin promotes direction sensing during collective cell migration. *Cell*, 157(5):1146–1159, 2014.
- [CV15] Andrew G Clark and Danijela Matic Vignjevic. Modes of cancer cell invasion and the role of the microenvironment. *Curr Opin Cell Biol*, 36(13–22):10–1016, 2015.
- [DRSB<sup>+</sup>05] Olivia Du Roure, Alexandre Saez, Axel Buguin, Robert H Austin, Philippe Chavrier, Pascal Siberzan, and Benoit Ladoux. Force mapping in epithelial cell migration. *Proceedings of the National Academy of Sciences*, 102(7):2390–2395, 2005.
- [FG09] Peter Friedl and Darren Gilmour. Collective cell migration in morphogenesis, regeneration and cancer. *Nature reviews Molecular cell biology*, 10(7):445–457, 2009.
- [FNW<sup>+</sup>95] Peter Friedl, Peter B Noble, Paul A Walton, Dale W Laird, Peter J Chauvin, Roger J Tabah, Martin Black, and Kurt S Zänker. Migration of coordinated cell clusters in mesenchymal and epithelial cancer explants in vitro. *Cancer research*, 55(20):4557–4560, 1995.
- [FOBS14] Alexander G. Fletcher, Miriam Osterfield, Ruth E. Baker, and Stanislav Y. Shvartsman. Vertex models of epithelial morphogenesis. *Biophysical Journal*, 106(11):2291–2304, 2014.
- [GT18] Matthew Good and Xavier Trepat. Cell parts to complex processes, from the bottom up, 2018.
- [Her32] Earl H Herrick. Mechanism of movement of epidermis, especially its melanophores, in wound healing, and behavior of skin grafts in frog tadpoles. *The Biological Bulletin*, 63(2):271–286, 1932.

- [Hol14] SJ Holmes. The behavior of the epidermis of amphibians when cultivated outside the body. *J. exp. Zool.*, 17(2):281–295, 1914.
- [HV23] Lea Happel and Axel Voigt. Coordinated motion of epithelial layers on curved surfaces. *Cluster of Excellence, Physics of Life, TU Dresden*, 2023.
- [JGS18] Frank Jülicher, Stephan W Grill, and Guillaume Salbreux. Hydrodynamic theory of active matter. *Reports on Progress in Physics*, 81(7):076601, 2018.
- [MJR<sup>+</sup>13] M Cristina Marchetti, Jean-François Joanny, Sriram Ramaswamy, Tan- niemola B Liverpool, Jacques Prost, Madan Rao, and R Aditi Simha. Hydrodynamics of soft active matter. *Reviews of modern physics*, 85(3):1143–1189, 2013.
- [PJJ15] Jacques Prost, Frank Jülicher, and Jean-François Joanny. Active gel physics. *Nature physics*, 11(2):111–117, 2015.
- [RCCT17] Pere Roca-Cusachs, Vito Conte, and Xavier Trepat. Quantifying forces in cell biology. *Nature cell biology*, 19(7):742–751, 2017.
- [TWA<sup>+</sup>09] Xavier Trepat, Michael R Wasserman, Thomas E Angelini, Emil Millet, David A Weitz, James P Butler, and Jeffrey J Fredberg. Physical forces during collective cell migration. *Nature physics*, 5(6):426–430, 2009.
- [VT66] RB Vaughan and JP Trinkaus. Movements of epithelial cell sheets in vitro. *Journal of cell science*, 1(4):407–413, 1966.
- [WV21] Dennis Wenzel and Axel Voigt. Multiphase field models for collective cell migration. *Physical Review E*, 104(5):054410, 2021.